PHYSICAL REVIEW B VOLUME 27, NUMBER 12 15 JUNE 1983

Electronic structure of Ce and its intermetallic compounds

J. C. Fuggle, F. U. Hillebrecht, Z. Zołnierek,* and R. Lässer
Institut für Festkörperforschung der Kernforschungsanlage Jülich, D-5170 Jülich, West Germany

Ch. Freiburg
Zentralabteilung für Chemische Analyse der Kernforschungsanlage Jülich, D-5170 Jülich, West Germany

O. Gunnarsson
Max-Planck-Institut für Festkörperforschung, D-7000 Stuttgart 80, West Germany

K. Schönhammer
Institut für Theoretische Physik der Universität Hamburg, D-2000 Hamburg, West Germany
(Received 17 August 1982; revised manuscript received 10 January 1983)

We report the core-level x-ray photoelectron spectroscopy spectra of 30 intermetallic compounds of La and Ce. The results are discussed in the light of calculations using the Anderson impurity model of the $4f$ levels and including the degeneracy of the $4f$ levels. The comparison allows us to derive values for the coupling between the f levels and the conduction states Δ and the number of $4f$ electrons n_f. We find Δ to be up to ~ 150 meV in some Ce intermetallic compounds, and find n_f to range from ~ 0.8—1.1. We cannot reconcile the core-level results with the traditional promotional model in which Δ was assumed to be 10 meV or less and the f-electron count could range from 1 down to zero in Ce intermetallic compounds.

INTRODUCTION

In this paper we summarize evidence from core-level x-ray photoelectron spectroscopy (XPS),[1–14] which strongly suggests that the f-electron count in so-called "mixed-valence" intermetallic compounds of Ce is always greater than 0.8 and that the Ce f levels are more strongly hybridized with the other conduction states than previously thought. The interpretation of the data is based on recent numerical calculations[15] within an impurity model for the XPS, without which the conclusions made here would not be justified.

The results of our studies cast doubt on the accepted framework within which the electronic structure of Ce intermetallic compounds is often described. In this framework, the $4f$-electron count in Ce compounds was assumed to vary between 0 and 1 with the Ce $4f$ electron being "promoted" to the $5d\,6s$ conduction states in many compounds (hence the name "promotional model"). The schematics of this framework were elegantly summarized by Iandelli and Palenzona[16] in a diagram redrawn for Fig. 1. While some authors might argue for small changes in the boundaries of Fig. 1, the basic idea is that in Ce compounds with elements of regions A and B the Ce f electron can be partially promoted to the conduction states. The f-electron count would then be below 1 and as the f levels were thought to be narrow it would become sensible to describe these compounds as "configuration-fluctuation" or mixed-valence materials. On the basis of lattice constant, magnetic, and superconducting properties, adherents of the promotional model thought that in A-rich Ce compounds the f level was completely above E_F and was empty. As there would then be four conduction electrons per Ce atom these compounds were called quadrivalent. In the Ce compounds with the group-C elements the promotional model required no promotion of an f electron and the compounds were known as trivalent.

Over the years several authors have questioned the applicability of the promotional model to Ce and its compounds (see, e.g., Refs. 17—21) for, as shown in Ref. 15, many of the properties (e.g., magnetic susceptibilities and anomalous lattice constants) attributed to f-electron promotion may be due to hybridization between the f levels and the conduction states. We will show that it is hard to understand core-level spectroscopic results on the basis of the promotional model. Combination of our theoretical framework with the experimental results leads us to deduce f-electron counts of ~ 0.8—1.1 and significant hybridization widths. We will list values for f-electron counts and widths for about 20 Ce com-

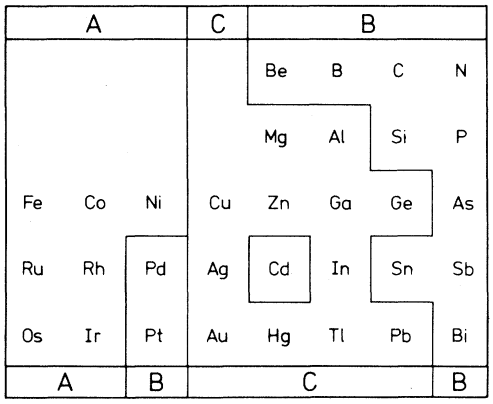

FIG. 1. Conventionally accepted categories of Ce compounds, for explanation see text. We will show that such a scheme is not helpful in the interpretation of XPS results and is in all probability wrong.

pounds and note here the need for common sense in using these numbers. On the one hand, they do depend on model calculations and should not be quoted dogmatically. On the other hand, the model used is physically reasonable and it seems unlikely that the values given are completely wrong and they should not be dismissed without reasonable grounds.

In order to ease interpretational problems we have studied both La and Ce compounds. The situation in core-level spectroscopy of these compounds is illustrated in Fig. 2. The spectroscopist can observe the energy of the transitions from the initial, ground state to several different core-ionized final states whose nominal f-electron counts are 0, 1, or 2.

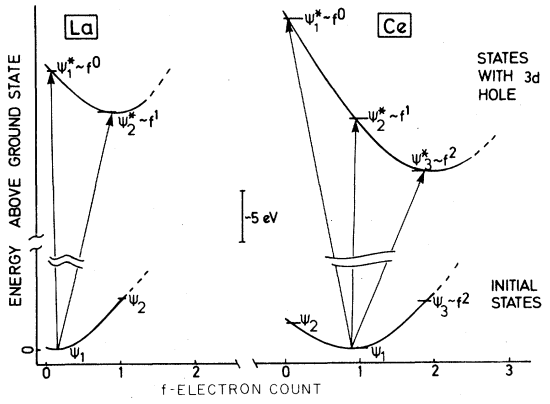

FIG. 2. Schematic diagram of $3d$ core-hole excitation in XPS of La and Ce compounds. Excitation takes place from an initial state into final states whose approximate configurations are $3d^9 4f^0$ and $3d^9 4f^2$.

From previous studies[1–11] the separations are known to be (in eV)

$$\epsilon_{f^0}-\epsilon_{f^1}\sim 11, \quad \epsilon_{f^1}-\epsilon_{f^2}\sim 4 \ .$$

The spectroscopist can also measure the relative intensities of these transitions and it is from these intensities that we derive values for the initial-state f-electron count and f-level hybridization. Following Refs. 11 and 15 we write the initial-state wave function Ψ_i as

$$\Psi_i=\sqrt{c_{(f^0)}}\phi_{(f^0)}+\sqrt{c_{(f^1)}}\phi_{(f^1)} +\sqrt{c_{(f^2)}}\phi_{(f^2)} \ , \tag{1}$$

where the $\phi_{(f^i)}$ are N-particle wave functions for the pure f^0, f^1, and f^2 configurations and the $c_{(f^n)}$ are the corresponding amplitudes. The weights $c_{(f^0)}$, $c_{(f^1)}$, and $c_{(f^2)}$ are, in general, not given directly by the relative intensities of the "f^0," "f^1," and "f^2" peaks spectroscopy[5,8,10,11] because there is some mixing of the final-state configurations as well as of the initial-state configurations. In a separate work, a theory has been developed to calculate the relative intensities of the XPS and Ce $3d$ x-ray–absorption spectroscopy (XAS) peaks as a function of the $(c_f i)$ and the hybridization Δ of the f electrons with the conduction states. Δ is defined as $\pi V^2\rho_{\max}$ where $\rho_{\max}$ is the maximum in the density of conduction states and V is the hybridization matrix element. The $c_{(f^i)}$ are varied by shifting the bare f-level position with respect to E_F. It is also necessary to choose values for U_{fc}, the Coulomb interaction between the core hole and the $4f$ subshell, and U, the Coulomb interaction between f electrons. These are not freely variable parameters, but are fixed using the separation of the core-level peaks in XPS and also the f^2 peak in bremsstrahlung isochromat spectroscopy.[22–24] In general, we used $U=6.40$ eV and $U_{fc}=9.6$ to 13.0 eV. The least important factor is the shape of the conduction-band density of states, which is estimated from XPS studies.[25] Here we use a semielliptical band with lower edge B^- and upper B^+ with respect to E_F. In general, the choice of B^- and B^+ is of secondary importance.

Figure 3 shows the calculated XPS spectra for a range of $c_{(f^0)}$ with $\Delta=120$ meV, which is near the upper limit of the hybridization suggested by our comparison with experiment. Note that the f-electron count (n_f) is not $1-c_{(f^0)}$ because of the contribution of the f^2 configuration. $c_{(f^2)}$ is always less than 0.05 in our calculations (it is largest for small $c_{(f^0)}$ and large Δ) and is probably not significant in most physical properties.

We discuss first the determination of $c_{(f^0)}$ from

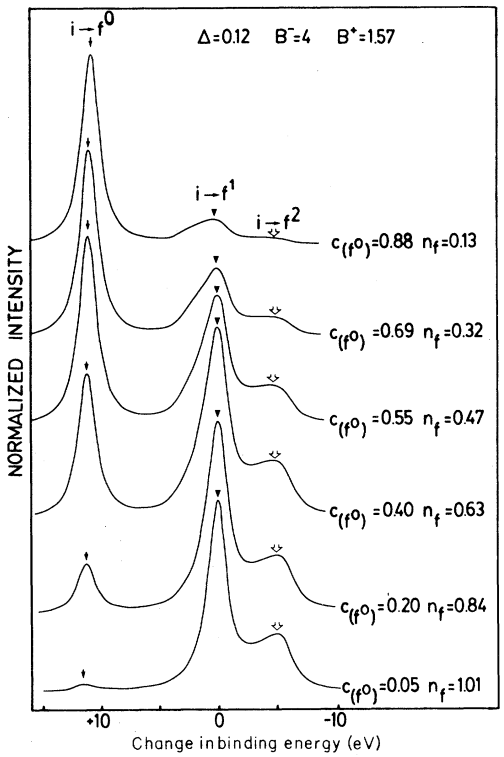

FIG. 3. Calculated Ce 3*d* XPS spectra with the ground-state weight of f^0 being varied parametrically.

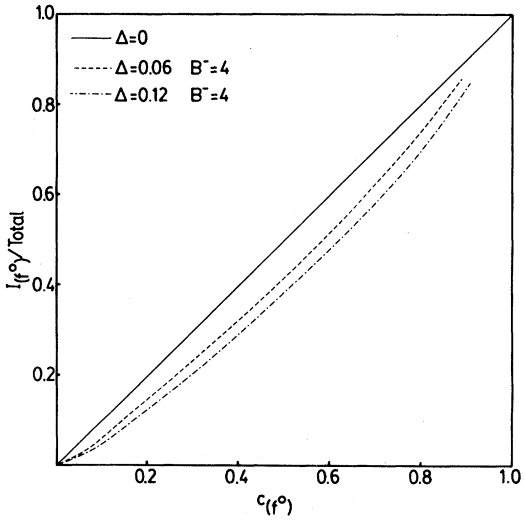

FIG. 4. Relative intensity of the f^0 peak in the calculated spectra as a function of the ground-state f^0 weight for three different values of hybridization between the f-electron level and the conduction states (given in eV). Weight of the f^0 peak was estimated using the same manual peak separation techniques as used later on the experimental spectra.

the intensity of the $i \rightarrow f^0$ XPS peak. It can be judged from Fig. 3 that the f^0 peak intensity does track $c_{(f^0)}$ quite well. The physics behind this is that distortion from proportionality is caused by final-state mixing of the f^0, f^1, and f^2 configurations. The energy of the f^0 configuration is approximately 11 eV above the f^1 configuration in the final state,[8–11,26] and is mixed with it only via the hybridization with the conduction states (with $N_f\Delta < 2$ eV, where N_f is the degeneracy of the f level). The final-state mixing is thus quite small and the deviation from proportionality of $c_{(f^0)}$ to the $i \rightarrow f^0$ peak intensity is not large. To illustrate this we applied a graphic peak separation procedure by hand to the calculated XPS spectra and plotted the relative area of the f^0 peak as a function of $c_{(f^0)}$ in Fig. 4. The deviation from proportionality is small, but not negligible, especially at very low weights of $c_{(f^0)}$. This is partly due to the peak separation procedure which involves drawing a line under the f^0 peak to remove the background. The procedures adopted underestimate the f^0 tails of the f^0 peaks, and small f^0 peaks can be lost in the background. In the theoretical calculation, the weight of the f^0 tails could be included but this would result in a poor simulation of experiment. Because of the problems with background subtraction and inelastic losses the XPS method is not reliable for determination of $c_{(f^0)}$ below 0.05. At higher values of $c_{(f^0)}$ the relative intensity of the f^0 peak $I_{(f^0)}$ in XPS will be up to 50% less than $c_{(f^0)}$ and the difference is larger for larger hybridization values.[27] For instance, with $\Delta = 120$ meV, a relative f^0 intensity of 0.2 would correspond to a $c_{(f^0)}$ of ~ 0.3. We feel such deviations justify previous caution about determination of the f-electron count from core-level spectra.[5,10,11] From the discussions of the f^0 peak, it is clear that the total weight of the f^1 and f^2 peaks is primarily determined by the f-level occupancy. The ratio $r = I_{(f^2)}/(I_{(f^1)} + I_{(f^2)})$, on the other hand, is dependent mainly on Δ, where $I_{(f^x)}$ is the weight of the f^x peak in the spectrum. This is illustrated in Figs. 5 and 6. The reason for this dependence is twofold. When Δ is increased, the final states (f^2) of primarily f^2 character hybridize more strongly with f^1 states. Since the f^1 final states have a relatively large overlap with the initial state, this leads to a larger weight of the f^2 peak. At the same time the increase of Δ increases the admixture, $c_{(f^2)}$, of f^2 states in the initial state. Since these f^2 states have a large overlap with the final f^2-like states, the weight of the f^2 peak is further increased. We can

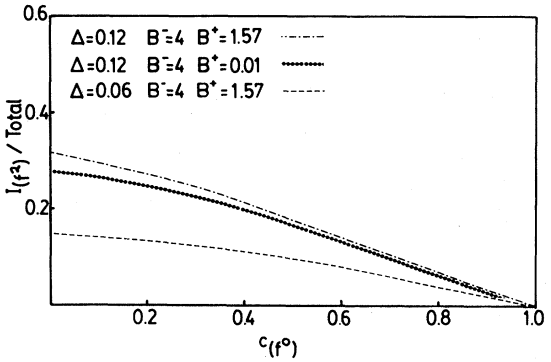

FIG. 5. Relative intensity of the f^2 peak as a function of the ground-state f^0 weight for two different values of Δ (the hybridization between the f levels and the conduction states) and different band parameters (all given in eV).

see from Fig. 6 that a change of Δ by a factor of 2 leads to a change of r by a factor of about 2 also. Thus r provides a sensitive measure of Δ. The dependence of r on other parameters, such as the f-level occupancy or the band parameters B^+ and B^-

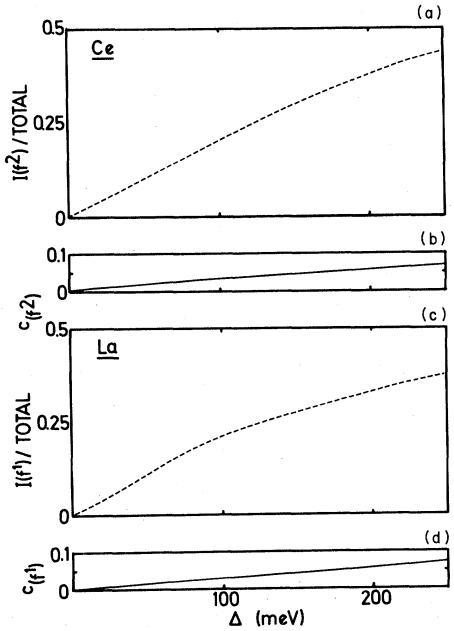

FIG. 6. Calculated variation of the weight of the "well-screened" f^{n+1} peaks as a function of the hybridization between the f level and the conduction states for La and Ce, also shown is the variation of $c^{(f^{n+1})}$. The semielliptical conduction band has $B^-=4$ eV, $B^+=1.57$ eV. For La the f-electron count is $c_{(f^1)}$, for Ce it was kept at 0.8.

is weaker. All the same, we note that the uncertainties in the conduction-band parameters, the estimates of the experimental peak weights, etc., as well as uncertainties in the model itself, mean that we should not be surprised if the Δ values given here differ by a factor of up to 2 from those found in other experiments. We will discuss the utility of such numbers later.

EXPERIMENTAL

The samples used in these studies were prepared by melting the components together in the required proportions using rf heating in a cold crubible. The metals used were of 99.99% purity or better, as specified by the procedures of Johnson and Matthey or Hereaus. The samples were brittle and mostly air sensitive. They were cut into 1.7-mm slices by spark erosion and checked for the presence of secondary phases by metallography and x-ray diffraction. If necessary the samples were annealed for up to a week *in vacuo* to reduce the concentration of peritectic precipitates. No samples on which data is reported here contained more than 5% of impurity phases. All samples were stored in Pyrex glass ampoules under vacuum or pure argon until use. Clean surfaces were obtained by scraping the samples *in vacuo* with an Al_2O_3 file. The level of O and C contamination, as judged by the O 1*s* and C 1*s* XPS peak intensities, did not exceed 5 at. % in the surface region. Further discussion of surface effects is given in the Appendix. The measurements were made in a ultrahigh-vacuum (UHV) photoelectron spectrometer custom built by Kratos Ltd. (United Kingdom). The instrument has typical operating pressures of 5×10^{-11} Torr in both measurement and sample preparation chambers. Al$K\alpha$ x rays from a homemade monochromator were used to excite the spectra. This monochromator has 54 quartz single crystals on a 1-m-radius toroidal substrate to utilize a large solid collection angle. In order to increase intensity the slits in the electron optics were opened which gave 600 meV total instrumental resolution. Reflection electron energy loss spectra were obtained by bombarding the samples with a primary beam from a Vacuum Generators model LEG-22 electron gun and energy analyzing the (nonspecular) backscattered electrons.

RESULTS AND DISCUSSION

La-Ni and Ce-Ni intermetallic compounds

Figure 7 illustrates the Ce 3*d* XPS spectra form $CeNi_5$. The $\sim$18-eV spin-orbit splitting of the 3*d* levels leads us to see six features, instead of just three as in the calculated spectrum of Fig. 3. In the

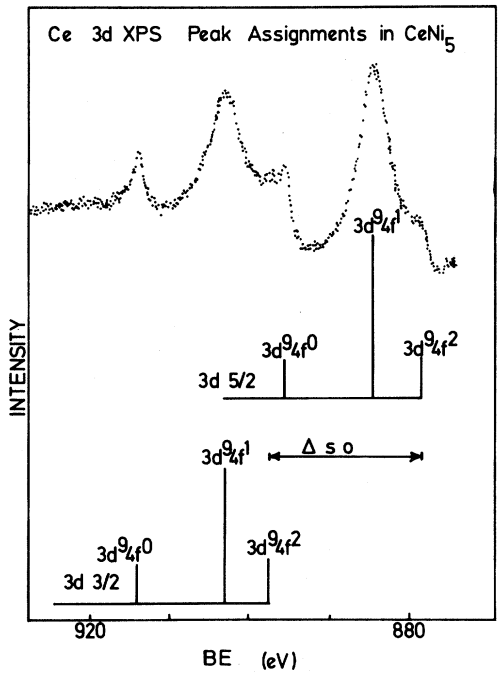

FIG. 7. 3*d* XPS spectrum of $CeNi_5$ with peak assignments.

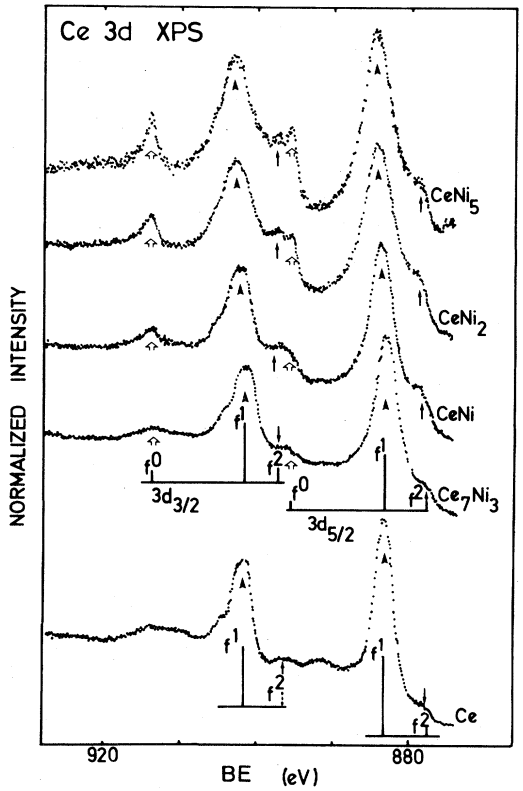

FIG. 8. 3*d* XPS spectra of the series of ordered Ce-Ni intermetallic compounds studied. Note the growth of the f^0 peaks with increasing Ni content.

case of Ce the $3d^9\ f^0$ and $3d^9\ f^2$ peaks strongly overlap, so that the $3d_{3/2}\ f^0$ peak must be used to estimate f^0 peak intensities. We multiply its measured intensity by $\frac{3}{2}$ to allow for the 6:4 ratio of the $3d\ \frac{5}{2}:\frac{3}{2}$ intensity ratios in order to make a comparison with the $\frac{5}{2}$ peaks.

The Ce 3*d* spectra from Ce-Ni intermetallics are presented in Fig. 8 and here the f^2 peaks grow in relative intensity as the Ni concentration is increased, indicating increased hybridization of the *f* levels. In the $CeNi_x$ compounds the f^0 peaks become distinct when $x > 1$ and increase in intensity as the Ni concentration increases. Before proceeding it is worth noting that the 4*d* XPS spectra of these Ce alloys contain strong evidence for the assignment of the peak at 914 eV to $3d^9 4f^0$ final states. The $CeNi_x$ spectra in Fig. 9 have intensity due to the $4d^9 4f^1$ and $4d^9 4f^2$ final states and Ni 3*s* ionization in the region between 105 and 115 eV binding energy (BE). In addition, two weak peaks grow up at 120 eV in the Ce compounds with high Ni concentration. Their splitting is almost equal to the 4*d* spin-orbit splitting in La (Ref. 1) so that they are unquestionably due to $4d^9 4f^0$ final states. The growth of the 3*d* peaks at 914 eV parallels the growth of the $4d^9 4f^0$ peaks at 120 eV and their separation from the main $d^9 f^1$ peaks is similar. Thus the 914-eV peaks can safely be assigned to excitations to final states mainly $3d^9 4f^0$ in character. The shape of the $4d^9 4f^1$ and $4d^9 4f^2$ region cannot be interpreted in detail because the 4*d*-4*f* interaction is strong and introduces strong multiplet effects in the 4*d* XPS peaks with complicated peak shapes that must be treated in intermediate coupling.

In Table I we present the energies of the 3*d* XPS peaks corresponding to f^0, f^1, and f^2 final states for the La and Ce compounds. It is noteworthy that the f^n-f^{n+1} peak separation remains constant in the La-Ni and Ce-Ni intermetallic compounds, but as will be seen later it varies as a function of stoichiometry in the Pd compounds. Table II gives the relative intensities of the peaks.

La and Ce intermetallic compounds with Pd and Sn

The anomalous properties of $CePd_3$ are often attributed to mixed valence.[6,23,28–34] $CeSn_3$ also has many unusual properties that are not well understood and have been attributed to mixed valence[23,28–38] and the compound does have a lattice constant anomaly.[35] These materials are thus suitable candidates for studies of group-*B* compounds.

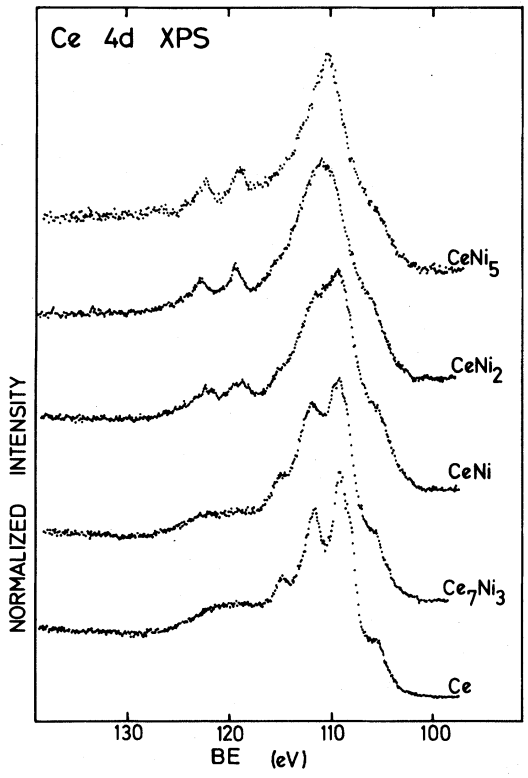

FIG. 9. $4d$ XPS spectra of the series of ordered Ce-Ni intermetallic compounds studied. Structure between 105 and 115 eV in Ce is due to the $4d^9$-$4f^1$ multiplet interaction. This distorts as the $4f$ hybridization is increased but, in addition, the Ni $3s$ peak at 110 eV provides $\sim 30\%$ of the total peak intensity in $CeNi_5$ due to the $4d^9 4f^0$ final states.

Figure 10 shows the $3d$ XPS spectra of $CePd_x$ intermetallic compounds. We assign the component at smaller BE to a transition to the final state with an f-electron count increased by approximately 1 compared with the ground-state configuration. The relative weight of this component increases with increasing Pd concentration, both in $LaPd_x$ and $CePd_x$ compounds. We interpret the increase to be due to increased hybridization of the f electrons with the valence electrons, in accord with Figs. 5 and 6.

All spectra were reproducible except the $CePd_3$ spectrum, which is the most interesting; it has a small peak at 914.7 eV which we attribute to f^0-like final states. In some cases the f^0 peak was broadened and the f^2 peak less sharp. We tentatively attribute this variation to small quantities of hydrogen in the sample because ~ 1 at. % hydrogen could be degassed from many samples by heating to 600 °C, and there may have been some surface segregation of the hydrogen. The main source of hydrogen seem to be the impurities in the initial Ce, cracking of hydrocarbons in the spark erosion process, and hydrogen produced by reaction with atmospheric water. The spectrum shown is that from a sample made with high purity Ce from Ames Laboratory and with minimum exposure to air and moisture. We do not have equipment, like SIMS (stimulated ion-mass spectroscopy) to monitor the surface hydrogen concentration but it would be interesting to investigate the surface hydrogen concentration as a function of temperature to check if it could explain the anomalous temperature dependence of the XPS spectra.[39]

Figure 11 contains expanded plots of the La and Ce $3d_{5/2}$ peaks from the La-Pd and Ce-Pd intermetallics. Although the f^n and f^{n+1} peaks overlap it is clear that their separation is not constant, but first decreases and then increases with increasing Pd concentration. The Ce peak widths are larger than those for La and the peaks broader with increasing Pd content. These shifts and broadening are due to multiplet effects[40] and a special broadening mechanism related to virtual-bound-state effects. These effects will be discussed in more detail elsewhere.[41]

Plasmon effects, shown in the XPS spectra of $CeSn_3$ and $LaSn_3$ in Fig. 12 were identified by comparison of the La or Ce and Sn XPS peaks. A plasmon loss of ~ 14 eV is observed on the Sn peaks from the compounds so that plasmon loss satellites of the $3d^9 4f^1$ peaks explain most of the intensity where the Ce $3d^9 4f^0$ peaks are normally found in $CeSn_3$. We cannot rule out a small $4f^0$ contribution but there is certainly not a large one. The most noticeable feature of the spectra in Fig. 12 is the very large increase in width of the peaks in $CeSn_3$. We believe this is again related to virtual-bound-state broadening[41] and makes it difficult to estimate accurately the relative intensity of the f^1- and f^2-like peaks in the spectrum, but the f^2 peak intensity seems only a little larger than in Ce metal itself.

Compounds with group-A elements: Au and Al

It is not necessary to show all the $CeAu_x$ and $CeAl_x$ spectra here, but the peak binding energies and relative peak intensities are given in Tables I and II. All the group-A compounds showed no detectable $3d^9 4f^0$ peaks and only weak $3d^9 4f^2$ peaks. We choose to illustrate the $CeAl_2$ spectrum in Fig. 13 because this shows only weak virtual-bound-state broadening. The f^1 and f^2 peaks are clearly separated and the f^1 peak is nearly as narrow as in Ce itself. The relative intensity of the f^2 peak is of the same order as Ce itself [differences are not larger than the accuracy of the deconvolution but in

TABLE I. $3d$ XPS peak binding energies for Ce intermetallic compounds (all values in eV with respect to E_F). Typical accuracies for $3d_{3/2}$ f^0,f^1 ~0.2–0.4 eV; for f^2, 0.5–1.0 eV; and for $3d_{5/2}$ f^0, f^2 ~0.5–1.0 eV (see Ref. 1 for more details).

	$3d_{3/2}$			$3d_{5/2}$			
	f^0	f^1	f^2	f^0	f^1	f^2	$\delta_{f^0-f^1}$
Ce		901.7	(896.4)		883.7	878.5	
$CeCo_2$	913.8	902.9	897.0	895.4	884.4	878.9	10.9
$CeCo_5$	914.1	902.8	897.8	895.4	884.4	879.3	11.1
Ce_7Ni_3		902.3	896.8		883.9	878.6	
CeNi	913.8	902.4	896.3		884.0	878.5	11.4
$CeNi_2$	914.0	903.0	897.4	895.6	884.5	878.8	11.0
$CeNi_5$	913.9	903.1	898.0	895.8	884.6	878.9	10.8
$CeRu_2$	914.0	903.2	896.1	895.7	884.8	878.9	10.8
Ce_7Pd_3		902.7	(896.6)		884.2	878.2	
CePd		903.1	898.8		884.6	879.8	
Ce_3Pd_5		903.0	898.7		884.6	879.9	
$CePd_3$	914.7	902.9	898.5		884.3	879.6	11.8
$CeSn_3$		902.9			884.6	878.0	
$CePt_3$	915.1	903.4	899.3	897.0	885.0	879.7	11.8
CeAu		903.0	896.4		884.4	877.7	
$CeAu_2$		903.2			884.7	878.1	
$CeAl_2$		901.9			883.5	877.8	
CePdAl		902.5	896.5		884.0	878.0	
$CeCu_2Si_2$[a]		902.1	897.3		883.6	878.8	
CeSe[a]		903.9	899.6		885.3	879.8	

[a]Reference 5.

the analogous Th compound XPS line-shape analysis suggests that the f levels are even more decoupled in $ThAl_2$ than in Th (Ref. 6)]. Plasmon loss features dominate the region where the $3d^9 4f^0$ peak would be found so that nothing can be said about the f^0 peaks in $CeAl_2$ except that they are not very large (i.e., ~10%).[5]

DISCUSSION

We first of all consider the problem of f-electron counts and the f^0 peaks. In all cases, only the $3d_{3/2}$ f^0 peak intensities can be accurately estimated; the $3d_{5/2}$ f^0 peak overlaps the $3d_{3/2}$ f^2 peak. We thus multiplied the $3d_{3/2}$ f^0 peak by $\frac{6}{4}$ to compare with the $3d_{5/2}$ f^1 and f^2 peaks. The relative f^0 intensities never reached more than ~16% in all the alloys studied, so that even after correction using Fig. 4, we only find $c_{(f^0)}$ values ranging up to ~0.26. This is in marked contrast to much of the traditional literature which gave f-electron–count values down to 0 or 0.2 (i.e., $c_{(f^0)}=0.8$ to 1.0) for many of the alloys studied, like $CeCo_2$, $CeNi_2$, or $CeRu_2$ (Refs. 16 and 28–34). We cannot rule out some contribution from surface effects in XPS. However, we can use the fact that the kinetic energy of the $4d$ photoelectrons is larger than the $3d$, so that they have a larger intensity. In general, the f^0 peak intensities are lower for $4d$ than for $3d$ spectra (see Table II). This discrepancy is probably due to difficulties in background subtraction, but the low $4d$ f^0 peak intensity does mean that the bulk Ce f-electron count cannot be substantially lower than at the surface. This is in accord with a similar conclusion reached by Krill *et al.* from comparison of XPS and x-ray absorption spectra.[7–9]

The size of the hybridization between the f electrons and the conduction states Δ can be estimated from the f^2 peak intensities with the use of Figs. 5 and 6. As described by Fig. 5, the f^2 peak intensity is mainly dependent on the value of Δ, but there is a secondary dependence on the shape of the valence band. This latter arises because the ground-state f^2 mixing with the valence states decreases with increasing separation from the bare f^2 position. Thus states just below E_F contribute more to the f^2 XPS peak than states at the bottom of the valence band. It is possible for us to use more realistic densities of states in the calculation of Δ than a semiellipse. For instance, we simulated the measured XPS valence bands for certain especially important examples in Ref. 42. However, in order to represent the general trends we find it more appropriate to use a simple semiellipse with $B^-=4$ eV and $B^+=1.57$ eV. Sub-

TABLE II. Relative intensities of peaks due to f^0, f^1, and f^2 final states in La 3*d*, Ce 3*d*, and Ce 4*d* XPS spectra (all values normalized to give total intensity equal to 1.0; comparisons between compounds are reliable to ~10%, absolute values depend on deconvolution procedure).

Compound	La 3*d* f^0:f^1	Ce 3*d* f^0:f^1:f^2	Ce 4*d* f^0:(f^1+f^2)
R	0.83:0.17	<0.04:0.92:0.08	<0.03:1.0
αCe [a]			<0.03:0.97
$CeCo_2$		0.10:0.65:0.25	
$CeCo_5$		0.07:0.70:0.23	
R_3Ni	0.82:0.18		
R_7Ni_3	0.8:0.20	<0.04:0.85:0.15	<0.03:1.0
*R*Ni	0.74:0.26	0.02:0.82:0.16	0.03:0.97
RNi_2		0.06:0.72:0.22	0.05:0.95
RNi_5	0.69:0.31	0.12:0.72:0.17	0.06:0.94
R_7Pd_3	0.88:0.12	<0.04:0.93:0.07	<0.03:1.0
*R*Pd	0.71:0.29	<0.04:0.80:0.20	<0.03:1.0
Ce_3Pd_5		<0.04:0.74:0.26	<0.03:1.0
$LaPd_2$	0.69:0.31		
RPd_3	0.58:0.42	0.05:0.65:0.30	~0.04:0.96
$CeRu_2$		0.12:0.61:0.27	~0.06:0.93
$CeRh_3$ [b]		~0.16:0.53:0.32	~0.07:0.93
RSn_3	0.83:0.17	<0.06:0.94:0.06	<0.06:1.0
$CePt_3$		0.07:0.64:0.29	
*R*Au	0.92:0.08	<0.04:0.94:0.06	<0.03:1.0
RAu_2	0.93:0.07	<0.04:0.97:0.03	<0.03:1.0
RAl_2		<0.10:0.93:0.07	<0.10:1.0
*R*PdAl	0.83:0.17	<0.10:0.91:0.09	<0.03:1.0
$CeCu_2Si_2$		<0.04:0.91:0.09	<0.03:1.0

[a]Reference 12.
[b]Reference 9.

stitution of the true density of states would normally change the deduced values of Δ by less than 30%. The weight of the f^2 peak also depends on the separation between the f^1 and f^2 states.

The values of Δ and $c_{(f^0)}$ deduced with the use of Figs. 5 and 6 and the observed spectra are listed in Table III, along with those deduced from previously published data from Refs. 4 and 5. As previously found,[6,10] the hybridization tends to be smaller in Ce than in La compounds because the Ce 4*f* orbitals are more contracted. The decrease is usually (30—50)%. Using data for the RPd_3 alloys from Ref. 10, we also estimate about a 50% decrease from Ce to Pr and from Pr to Nd. The Ce average distance increases with increasing dilution of Ce. Thus the increase of Δ with increasing Ni or Pd concentration is a strong indication that the *f* hybridization arises from overlap with Ni or Pd *d* orbitals on the neighboring atoms rather than *f*-*f* overlap.

In our opinion no experiment, least of all valence-band photoemission,[42] measures the size of hybridization of the 4*f* levels with the conduction states directly. Nevertheless, both valence-band (see, e.g., Refs. 43—48) and core-level studies are in accord in their indication that the hybridization is not as small as indicated by experiments which probe the spin dynamics of the *f* electron (e.g., neutron scattering[49] or time-dependent perturbed angular distribution of γ rays[50]). The latter probes the spin-flip times while we probe the total hybridization. It is of interest that although the absolute values of Δ deduced from our experiments and those on spin dynamics differ by at least a factor of 10, there are similarities in trends. For instance, we find Δ to be reduced by a factor of 5 between $CeSn_3$ and $CeAu_2$, while Riegel *et al.* find the spin dynamics for Ce in Au to be 3 times slower for Ce in Au than for Ce in Sn.[50]

The interplay of hybridization and *f*-electron—count effects is important for determination of *f*-electron counts from lattice constants. In doing this it was until now assumed that the lattice constant varied linearly with *f*-electron count between the value for 3^+ Ce(f^1) and 4^+ Ce(f^0), as shown in Fig. 14. This assumed that the *f*-electron hybridization energy was negligible so that, for in-

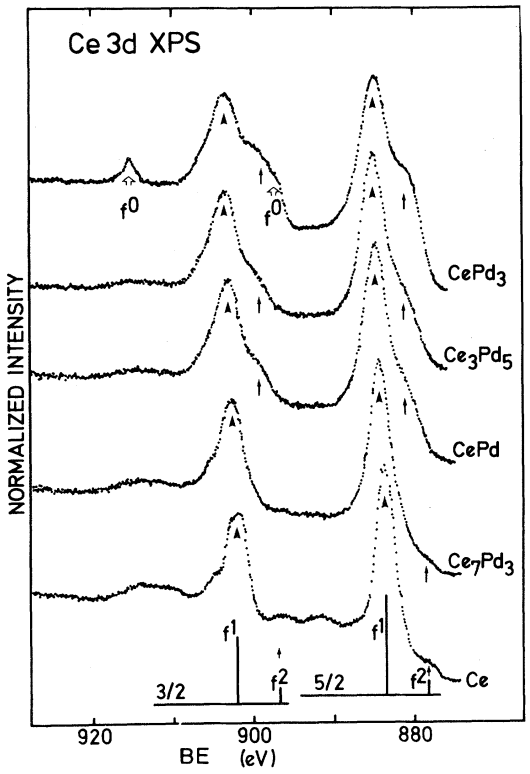

FIG. 10. 3*d* XPS spectrum of the ordered Ce-Pd intermetallic compounds studied.

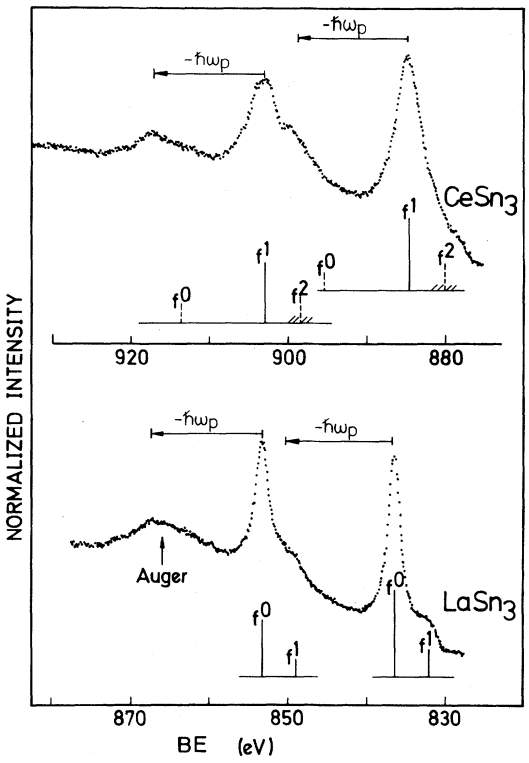

FIG. 12. 3*d* XPS spectra from $LaSn_3$ and $CeSn_3$.

stance, if the lattice constant was halfway between that for an f^0 and f^1 compound, then one would deduce a $c_{(f^0)}$ value of 0.5 as indicated by the dash-dot line in Fig. 14. Apart from the difficulty of deciding on a lattice constant for Ce f^0 materials the large values of the hybridization suggested by our XPS results would probably give a significant contribution to the cohesion of the alloy. This would reduce the lattice constant by an amount that is hard to estimate, but as shown schematically by the dashed curve in Fig. 14, the effect would lead to a systematic reduction of the values of $c_{(f^0)}$ derived from lattice constant data.

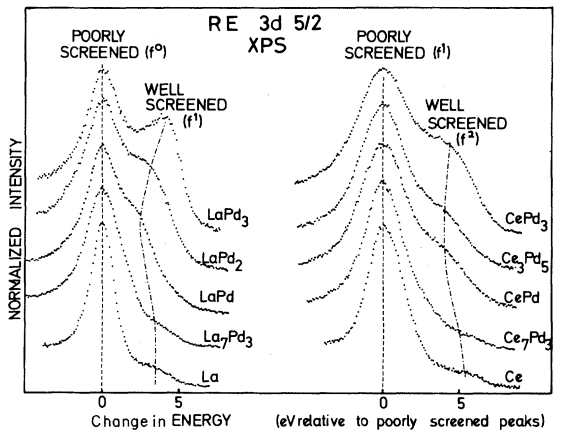

FIG. 11. Main $3d_{5/2}$ XPS peak from La-Pd and Ce-Pd intermetallic compounds.

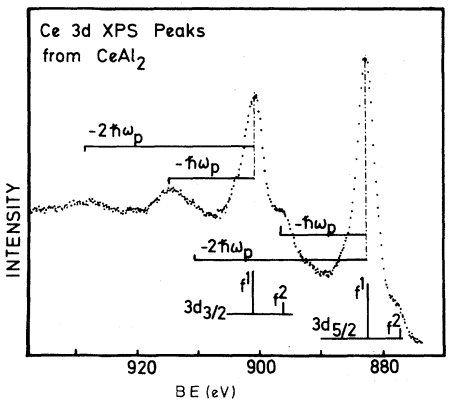

FIG. 13. 3*d* XPS spectrum from $CeAl_2$, with associate plasmon losses.

TABLE III. $4f$ Hybridization widths in meV and $c_{(f^0)}$ coefficients for La and Ce compounds.

Compounds	Δ_{4f}(La) from XPS	$\Delta_{4f}(Ce)$ from XPS	$c_{(f^0)}$(Ce) from XPS
R	70	30	<0.05
αCe[a]			~ 0.05
$CeCo_2$		120	~ 0.18
$CeCo_5$		110	~ 0.13
La_3Ni	80		
R_7Ni_3	90	60	<0.05
RNi	120	70	~ 0.05
$CeNi_2$		100	~ 0.12
RNi_5	160	70	~ 0.16
$CeRh_3$[b]		160	~ 0.26
$CeRu_2$		120	~ 0.20
R_7Pd_3	50	30	<0.05
RPd	140	90	<0.05
Ce_3Pd_5		120	<0.05
$LaPd_2$	160		
RPd_3	250	150	~ 0.10
RSn_3	70	50	<0.05
$CePt_3$		150	~ 0.14
RAu	30	25	<0.05
RAu_2	25	15	<0.05
$CeAl_2$		30	<0.05
RPdAl	70	35	<0.05
$CeCu_2Si_2$		35	<0.05
CeN			~ 0.2
CeSb		60	<0.05
CeSe		140	<0.05

[a]Reference 12.
[b]Reference 8.

CONCLUDING REMARKS

We have used core-level XPS to derive a set of values for the strength of hybridization between the Ce $4f$ levels and the conduction states and for the contribution of the $4f^0$ configuration to the ground state in Ce intermetallic. A certain amount of common sense is regarded in their use. On the one hand, they are not without a good theoretical foundation. On the other hand, they are only as good as the model used to extract them and should not be taken as a new dogma. We should be most pleased if other workers were to use the parameters we derive as starting values in calculations of other physical properties of Ce intermetallics. The clear message of our data is that theories utilizing very small (<10 meV) total $4f$ hybridization widths for Ce are not appropriate for describing the physical properties of Ce intermetallics. Further, we find f-electron counts greater than ~ 0.8 in all compounds studied and cannot reconcile the concept of small f-electron counts within the model used. We also believe that the data in Table III can be useful in design of experiments. For instance, if one wanted to compare the properties of Ce compounds with very different $4f$ hybridization widths Table III gives a reasonable guide to the choices available.

Another direction of study suggested by our work would be investigation of the role of the density of states near E_F in different experiments. The hybridization measured by the f^2 XPS peak is only weakly weighted to favor the effects of states near E_F. In contrast, resistivities and electronic specific heats are more strongly influenced by the states near E_F. In $CePd_3$, the density of sd states at E_F suggested by XPS is less than $\frac{1}{20}$ of the maximum, so that hybridization with states close to E_F is very small. In $CeSn_3$, the density of states near E_F suggested by XPS valence-band studies is near to the maximum in the band. Thus although the $CeSn_3$ f-electron conduction-band hybridization given in Table I is less than for $CePd_3$, the hybridization with states close to E_F must be larger than in $CePd_3$. Such effects must clearly be taken into account in calculating properties of Ce compounds which are related to a small perturbation of the ground state.

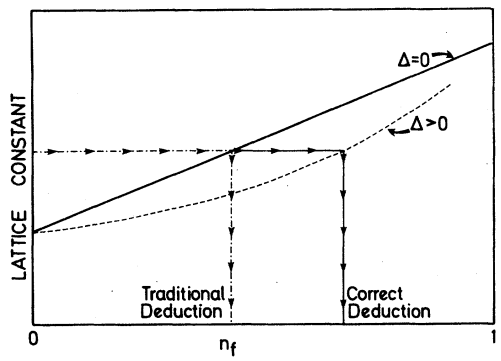

FIG. 14. Illustration of the effect of hybridization on the derivation of f-electron counts from lattice constants.

ACKNOWLEDGMENT

We thank Professor M. Campagna for his support of this work, as well as M. Beyss and J. Keppels for invaluable technical assistance. We are also grateful to J. Allen, Y. Baer, A. Bringer, G. Krill, S.-J. Oh, G. A. Sawatzky, and D. Wohlleben for stimulating discussions.

APPENDIX: SURFACE EFFECTS

What follows is a short discussion of the present status of surface effects in photoelectron spectra and possible artifacts of the sample cleaning methods used. The main thrust of this discussion will be that while it would be pointless to argue that no surface effects are present, they do not dominate the effects

we have observed.

The inelastic mean free path of electrons with ~600 eV kinetic energy (KE) is about 10 Å (Refs. 51 and 52) so that, even with almost vertical takeoff for the electrons as used here, approximately 20% of the spectrum arises from the first atomic layer where the Ce electrons might have different f-electron count and electronic structure. However, as pointed out by Krill *et al.*,[8] surface effects cannot dominate XPS results because similar variations are found in x-ray absorption studies, which are not strongly surface sensitive. Note also that the f-electron count and f-electron hybridization effects derived from our XPS measurements also allow us to rationalize synchrotron photoemission spectra of Ce valence bands in which the photoelectron KE was only 40—120 eV and surface sensitivity was even greater.[15,42] The implication is that if surface effects are localized at the surface, and measurements using ~10- and ~3-Å mean free paths give consistent results, then the first atomic layer is quite similar to all the rest.

Surface segregation can be a problem in photoemission studies. This is partially alleviated in ordered intermetallic compounds where the energy loss due to breakdown of the (thermodynamically very stable) compound is larger than the energy gain due to drop in surface energy when the more volatile component segregates to the surface.

We chose to clean the surfaces by filing *in situ,* rather than ion etching, to avoid the effects of selective sputtering on the surface composition. We checked the surface compositions in selective cases using the relative intensities of the core-level peaks from the two components and tabulations of photoionization cross sections. This showed the absence of any gross changes in surface composition.

The use of filing may conjure up a picture of rough, craggy surfaces covered in debris, and possibly atomically very rough. The samples used here mostly cleaved easily so that most of the surfaces examined consisted of small flat planes 0.1—1 mm^2 in area and oriented at ±20 deg to the average surface. We examined a few samples under a microscope and found that less than 10% of the surface was covered by debris. There was more powdery material on the surface of rare-earth rich intermetallics like Ce_7Ni_3 or $LaPd_3$, but these oxidized too rapidly for microscopic analysis. It is not possible to examine the surfaces for roughness on the atomic scale, but under the highest optical resolution possible in our reflection microscopes the individual cleavage faces showed little structure other than a few long straight steps.

---

*Present address: Institute for Low Temperature Studies, 50-950 Wroclaw, Poland.

[1]The XPS spectra reported here are drawn from a very extensive study of La intermetallic compounds and Ce intermetallic compounds which has been published. That study contained extensive investigations to rule out possible spurious effects like inelastic scattering and virtual-bound-state broadening in the final state. As that study included much that was of only peripheral interest in the central theme of this paper, it has been prepared separately as an unpublished Kernforschungsanlage (KFA) report by J. C. Fuggle, F. U. Hillebrecht, Z. Zołnierek, R. Lässer, and Ch. Freiburg, No. 1824 (unpublished). Further copies are available from the authors, or the Kernforschungsanlage Jülich librarian. Other important XPS studies of core levels are in Refs. 2—11.

[2]G. K. Wertheim, and M. Campagna, Solid State Commun. 26, 553 (1978).

[3]G. Crecelius, G. K. Wertheim, and D. N. E. Buchanan, Phys. Rev. B 18, 6519 (1978).

[4]Y. Baer, R. Hauger, Ch. Zürcher, M. Campagna, and G. K. Wertheim, Phys. Rev. B 18, 4433 (1978).

[5]R. Lässer, J. C. Fuggle, M. Beyss, M. Campagna, F. Steglich, and F. Hulliger Physica (Utrecht) 102B, 360 (1980).

[6]J. C. Fuggle, M. Campagna, Z. Zołnierek, R. Lässer, and A. Platau, Phys. Rev. Lett. 45, 1597 (1980).

[7]G. Krill, L. Abadli, M. F. Ravet, J. P. Kappler, and A. Meyer, J. Phys. (Paris) 41, 1121 (1980).

[8]G. Krill, J. P. Kappler, A. Meyer, L. Abadli, and M. F. Ravet, J. Phys. F 11, 1713 (1981).

[9]G. Krill and J. P. Keppler, J. Phys. C 14, L515 (1981) and references therein.

[10]F. U. Hillebrecht and J. C. Fuggle, Phys. Rev. B 25, 3550 (1982).

[11]J. C. Fuggle, F. U. Hillebrecht, Z. Zołnierek, Ch. Freiburg, and M. Campagna, in *Valence Instabilities,* edited by P. Wachter and H. Boppart (North-Holland, Amsterdam, 1982), p. 267.

[12]R. A. Pollak, S. P. Kowalczyk, and R. W. Johnson, in *Valence Instabilities and Related Narrow Band Phenomena,* edited by R. D. Parks (Plenum, New York, 1977), p. 5027.

[13]L. Schlapbach and H. R. Scherrer, Solid State Commun. 41, 893 (1982); L. Schlapbach and J. Osterwalder, Solid State Commun. 42, 271 (1982).

[14]S.-J. Oh and S. Doniach, Phys. Rev. B 26, 2085 (1982). This pioneering paper gave the first quantitative estimates of the hybridization of f-level hybridization widths Δ from core-level peak intensities, as suggested by Ref. 6. The values of Δ given were too high because degeneracy could not be taken into account at that stage.

[15]O. Gunnarsson and K. Schönhammer (unpublished).
[16]A. Iandelli and A. Palenzona, *Handbook on the Physics and Chemistry of the Rare Earths,* edited by K. A. Gschneidner, Jr. and L. Eyring (North-Holland, Amsterdam, 1979), Vol. II, p. 1. See references herein for the origin of the promotional model of Ce and its compounds.
[17]B. Coqblin and A. Blandin, Adv. Phys. 17, 281 (1968).
[18]M. Maple and J. Wittig, Solid State Commun. 9, 1611 (1971); see also J. Wittig, in *Physics of Solids under High Pressure,* edited by J. S. Schilling and R. N. Shelton (North-Holland, Amsterdam, 1981), p. 283.
[19]B. Johansson, Philos. Mag. 30, 469 (1974).
[20]F. R. de Boer, W. H. Dijkman, W. C. M. Mattens, and A. R. Miedema, J. Less-Common Met. 64, 241 (1979); P. F. de Chatel and F. R. de Boer, p. 377 in Ref. 1.
[21]U. Kornstadt, R. Lässer, and B. Lengeler, Phys. Rev. B 21, 1898 (1980).
[22]J. K. Lang, Y. Baer, and P. A. Cox, J. Phys. F 11, 121 (1981).
[23]Y. Baer, H. R. Ott, J. C. Fuggle, and L. E. De Long, Phys. Rev. B 24, 5384 (1981).
[24]F. U. Hillebrecht and J. C. Fuggle (unpublished).
[25]J. C. Fuggle, F. U. Hillebrecht, R. Zeller, Z. Zołnierek, P. A. Bennett, and Ch. Freiburg, Phys. Rev. B 27, 2145 (1983); 27, 2179, (1983); 27, 2194 (1983).
[26]J. F. Herbst and J. W. Wilkins, Phys. Rev. B 20, 2999 (1979).
[27]For determination of n_f the value of $c_{(f^2)}$ is also important. It has been almost ignored until now, but as seen below $c_{(f^2)}$ can be as large as 0.05. Such a large $c_{(f^2)}$ would partially offset the error in assuming that the f^0 intensity equals $c_{(f^0)}$ if it were assumed that $n_f = 1 - c_{(f^0)}$.
[28]*Valence Fluctuations in Solids,* edited by L. M. Falicov, W. Hanke, and M. B. Maple (North-Holland, Amsterdam, 1981), and references therein.
[29]*Valence Instabilities,* edited by P. Wachter and H. Boppart (North-Holland, Amsterdam, 1982).
[30]C. M. Varma, Rev. Mod. Phys. 48, 219 (1975).
[31]A. Jayaraman, P. D. Dernier, and L. D. Longinotti, High Temp.-High Pressures 7, 1 (1975).
[32]J. M. Lawrence, P. S. Riseborough, and R. D. Parks, Rep. Prog. Phys. 44, 1 (1981), and references therein.
[33]H. Kirchmayr in *Handbook on the Physics and Chemistry of the Rare Earths* edited by K. A. Gschneidner, Jr. and L. Eyring (North-Holland, Amsterdam, 1979), Vol. II, p. 55.
[34]D. C. Koskenmaki and K. A. Gschneidner, in *Handbook on the Physics and Chemistry of Rare Earths,* edited by K. A. Gschneidner and L. Eyring (North-Holland, Amsterdam, 1979), Vol. I, p. 337.
[35]I. R. Harris, M. Norman, and W. E. Gardner, J. Less-Common. Met. 29, 299 (1972).
[36]I. R. Harris, M. Norman, and W. E. Gardner, J. Less-Common. Met. 29, 299 (1972).
[36]I. R. Harris and V. G. Raynor, J. Less-Common Met. 9, 7 (1965).
[37]S. H. Liu, C. Stassis, and K. A. Gschneidner, Jr., p. 99 in Ref. 1 and references therein.
[38]J. Lawrence and D. Murphy, Phys. Rev. Lett. 40, 961 (1978) and references therein.
[39]G. Krill, L. Abadli, M. F. Ravet, J. P. Kappler, and A. Meyer, J. Phys. (Paris) 41, 1121 (1980).
[40]J.-M. Esteva, R. C. Karnatak, J. C. Fuggle, and G. A. Sawatzky, Phys. Rev. Lett. 50, 910 (1983).
[41]G. A. Sawatzky, J. C. Fuggle, O. Gunnarsson, and K. Schönhammer (unpublished); see also K. Schönhammer and O. Gunnarsson, Solid State Commun. 23, 691 (1977); 26, 147 (1978); 26, 394 (1978); Z. Phys. B 30, 297 (1980).
[42]O. Gunnarsson, K. Schönhammer, J. C. Fuggle, F. U. Hillebrecht, and D. Hillebrand (unpublished).
[43]J. W. Allen, S.-J. Oh, I. Lindau, J. M. Lawrence, L. I. Johansson, and S. B. M. Hagström, Phys. Rev. Lett. 46, 1100 (1981).
[44]M. Croft, J. H. Weaver, D. J. Peterman, and A. Franciosi, Phys. Rev. Lett. 46, 1104 (1981).
[45]N. Martensson, B. Reihl, and R. D. Parks, Solid State Commun. 41, 573 (1982).
[46]D. J. Peterman, J. H. Weaver, and M. Croft, Phys. Rev. B 25, 5530 (1982).
[47]J. W. Allen, S.-J. Oh, I. Lindau, and M. B. Hagström, Phys. Rev. B 26, 445 (1982); J. M. Lawrence, J. W. Allen, S.-J. Oh, and I. Lindau, Phys. Rev. B 26, 2362 (1982).
[48]W. Gudat, M. Iwan, R. Pinchaux, and F. Hulliger, p. 249 in Ref. 29.
[49]E. Müller-Hartman, in *Electron Correlation and Magnetism in Narrow-Band Systems,* Springer Series in Solid State Sciences, edited by T. Moniya (Springer, Berlin, 1981), Vol. 29, and references therein.
[50]D. Riegel, H. J. Barth, M. Luszik-Bhadra, and G. Netz (unpublished).
[51]M. P. Seah and W. A. Dench, Surf. Interface Anal. 1, 2 (1979), and references therein.
[52]J. Szajman, J. Liesegang, J. G. Jenkin, and R. C. G. Leckey, J. Electron Spectrosc. Relat. Phenom. 23, 97 (1981), and references therein.